Vol 14 No 12, December 2005
1009-1963/2005/14(12)/2478-06
Chinese Physics
© 2005 Chin. Phys. Soc.
and IOP Publishing Ltd

Superexcited states of carbon monoxide studied by fast-electron impact*

Fan Lan-Lan(范岚岚)[a], Zhong Zhi-Ping(钟志萍)[b], Zhu Lin-Fan(朱林繁)[a]†,
Liu Xiao-Jing(刘小井)[a], Cheng Hua-Dong(成华东)[a],
Yuan Zhen-Sheng(苑震生)[a], and Xu Ke-Zun(徐克尊)[a]

[a] *Hefei National Laboratory for Physical Sciences at Microscale, Department of Modern Physics, University of Science and Technology of China, Hefei 230026, China*

[b] *College of Physical Science, Graduate School of the Chinese Academy of Sciences, Beijing 100049, China*

(Received 22 April 2005; revised manuscript received 8 August 2005)

Absolute optical oscillator strength density and double differential cross section spectra of CO below 120 eV are determined by fast electron impact. Some peaks above the first ionization threshold stand out as the momentum transfer square K^2 increases. The doubly excited Rydberg states converging to $C\ ^2\Sigma^+$, $D\ ^2\Pi$, and $F\ ^2\Pi$ states of CO^+, respectively, are confirmed in our spectra. Another peak at around 32 eV is assigned to the transition of $(3\sigma)^{-1}(2\pi)^1\ ^1\Pi \leftarrow X^1\Sigma^+$.

Keywords: oscillator strength, superexcited state, energy loss, CO
PACC: 3270C, 3150, 3450B

1. Introduction

The inelastic scattering of fast electrons provides a powerful means to measure absolute cross sections (optical oscillator strength (OOS) and generalized oscillator strength (GOS)) for dipole-allowed and dipole-forbidden transitions in atoms and molecules.[1] The double differential cross section (DDCS) $\mathrm{d}^2\sigma/(\mathrm{d}E\mathrm{d}\Omega)$ is related to the generalized oscillator strength density (GOSD) $\mathrm{d}f(E,K)/\mathrm{d}E$ in the framework of the first Born approximation by the Bethe–Born formula (in atomic units):[1,2]

$$\frac{\mathrm{d}f(E,K)}{\mathrm{d}E} = \frac{E}{2}\frac{p_0}{p_a}K^2\frac{\mathrm{d}^2\sigma}{\mathrm{d}E\mathrm{d}\Omega}. \qquad (1)$$

Here E and K are the excitation energy and momentum transfer, p_0 and p_a are the incident and scattered electron momenta, respectively. In the limit $K \to 0$, the GOSD is identical to the optical oscillator strength density (OOSD).

Absolute GOS values can be used to provide an effective feedback for the wavefunction of both the ground and excited states as well as evaluate and develop new quantum computational methods for the excited states.[1] In addition, the generalized oscillator strengths can be visualized in the form of the Bethe surface, i.e. a three-dimensional representation of the GOS as a function of the excitation energy E and the logarithm of the momentum transfer $\ln(K^2)$.[1] The Bethe surface embodies all the information concerning the inelastic scattering of electrons by an atom or molecule in the framework of the first Born approximation.[1] Furthermore, the K^2 dependence behaviours of the GOS may provide the quantitative information about spectral assignments, especially for superexcited states, i.e. the excited states of molecules above the first ionization threshold, such as high Rydberg states, doubly or inner-shell excited, non-Rydberg states, etc.[3–5] The very recent work[6–8] has elucidated that some weak dipole-allowed or dipole-forbidden superexcited states may stand out with the momentum transfer square K^2 increasing.

The ground state of CO can be written as $(1\sigma)^2(2\sigma)^2(3\sigma)^2(4\sigma)^2(1\pi)^4(5\sigma)^2$. Its valence shell excitations have been well studied, which were reviewed by Chan *et al.*[9] As for the energy levels

*Project supported by the National Nature Science Foundation of China (Grant Nos 10474089, 10134010 and 10004010).
†E-mail: lfzhu@ustc.edu.cn

above the first ionization threshold of CO, the superexcited states have been studied by the photoabsorption method,[10] the photoelectron spectroscopy (PES)[11] and the photo-induced dispersed fluorescence spectroscopy (PIFS),[12−16] such as the Rydberg series converging to $C^2\Sigma^+$ and $D^2\Pi$ of CO^+. Ion-yield curves, i.e. the intensities of O^- and C^- negative-fragment-ion as a function of the photon excitation energy, have also been measured to study the superexcited states in an energy range of 20–40 eV.[17] Some of the CO resonances were tentatively assigned to doubly excited Rydberg series converging to the $D\ ^2\Pi$, $E\ ^2\Sigma^+$, and $E'\ ^2\Sigma^+$ satellite states of CO^+.[17] On the other hand, the electron-energy-loss spectra below 55 eV of CO were measured by Lee[18] with a low energy resolution (2.5 eV) at a high incident electron energy (25 keV). Lee found that two peaks stood out at large momentum transfers. One was at around 22 eV, and it was supposedly related to two electron transitions. The other was broad peak at around 32 eV that was observed at large momentum transfers, and assigned to the inner-valence transition of $(3\sigma)^{-1}(2\pi)^1\ ^1\Pi \leftarrow X^1\Sigma^+$ or $(3\sigma)^{-1}(6\sigma)^1\ ^1\Sigma^+ \leftarrow X^1\Sigma^+$. Since the momentum transfer dependence behaviours may be different for different superexcited states, some states overwhelmed in the OOS density spectrum may stand out in the electron-energy-loss spectra at large scattering angles. Therefore, the angle-resolved electron-energy-loss spectroscopy (AREELS) with a high energy resolution may provide more information for the structures and nature of the superexcited states. This is our main interest in this paper.

In a similar way to our previous studies of NO, O_2 and N_2,[7,8,19] in this work we measure the electron-energy-loss spectra of CO with a higher energy resolution of 100 meV and in a larger momentum transfer region. Then the absolute OOSD and DDCS are determined. Some peaks above the first ionization threshold stand out at large scattering angles. Based on the previous work[10−16,18] and present results, these peaks are clearly assigned.

2. Experimental and theoretical methods

The angle-resolved electron-energy-loss spectrometer used in this experiment has been described in detail in Refs.[20–22]. Briefly, it consists of an electron gun, a hemispherical electrostatic monochromator made of aluminium, a rotatable energy analyser of the same type, an interaction chamber, a number of cylindrical electrostatic lenses, and a one-dimensional position sensitive detector for detecting the scattered electrons. All of these components are enclosed in four separate vacuum chambers made of stainless steel. The impact energy of the spectrometer can be varied from 1 to 5 keV. For the present experiment, it was set at 2.5 keV and the energy resolution was about 100 meV. All spectra were measured at a pressure of 8×10^{-3} Pa and the background pressure in the vacuum chamber was 5×10^{-5} Pa. The true zero angle was calibrated by the symmetry of the angular distribution of $C^1\Sigma^+, \nu' = 0 \leftarrow X^1\Sigma^+$[23] inelastic scattering signal around the geometry nominal 0°. The angular resolution was about 0.8° in present measurement.

The electron-energy-loss spectra of CO were measured in a scattering angle range of 0°–8° with an interval of 2°, and calibrated at 11.39 eV according to the transition to $C^1\Sigma^+, \nu = 0$.[23] Then, the spectrum measured at a mean scattering angle of 0° was converted into relative OOSD spectrum by multiplying the Bethe-Born conversion factor of the spectrometer.[22,24−26] The spectra at other scattering angles were converted into relative GOSD spectra according to Eq.(1).

These relative GOSD spectra were transformed into absolute ones by the valence shell Bethe sum-rule:[1,27]

$$S_{\mathrm{val}}(0) = N_{\mathrm{val}} + N_{\mathrm{PE}} = \int_{E'}^{\infty} \left(\frac{\mathrm{d}f}{\mathrm{d}E}\right) \mathrm{d}E, \qquad (2)$$

where N_{val} is the total number of valence electrons in the target (10 for CO), N_{PE} is a small correction (0.3 for CO) for the Pauli-excluded transitions from the K-shell to the already occupied valence shell orbitals,[28,29] and E' is the lowest excitation energy. In the limit $K \to 0$, the GOSD is identical to the OOSD. In the sum-rule normalization procedure, the intensity of the relative OOSD or GOSD obtained at a definite scattering angle was first numerically integrated over a sampling energy loss range, i.e. up to 73 eV for 0°, 107 eV for 2°, 4°, and 6°, 120 eV for 8°. The remaining intensity of the valence shell above the measured energy region was estimated by integrating a fitted function aE^{-b} with respect to E from the limit energy of the measurements to infinity, where the empirical parameters a and b were obtained by least-squares fitting a smoothly decreasing region, i.e. 50–73 eV for 0°, 50–107 eV for 2°, 60–107 eV for 4°,

80–107 eV for 6°, and 80–120 eV for 8°, respectively. The overall percent errors of the OOSD and DDCS obtained in this work are less than 20%, which mainly come from the angular determination, the angular correction factor, the statistics of counts, and the least-squares fitting procedure.

The multi-scattering self-consistent-field (MSSCF or MS-X_α) method was employed in this work. Briefly, based on a trial charge density of the molecule, a muffin-tin trial molecular potential $V^{\rm mol}$ with the symmetry of molecular point group was constructed. We can then calculate the occupied molecular orbitals (MOs), which served to construct the charge density of the molecule and then a new trial molecular potential. With this process going on, self-consistent iterations were performed until a certain precision was met. A self-consistent-field (SCF) molecular potential $V_{\rm scf}^{\rm mol}$ was obtained and thereafter we calculated all MOs, including nondiffusive molecular orbitals (NMOs), Rydberg molecular orbitals (RMOs), and adjacent continuum molecular orbitals (CMOs). In our calculations, all RMOs and CMOs were treated in a unified manner in the framework of Quantum Defect Theory (QDT).[30–34] With the calculated wavefunctions, the GOSD can be calculated. The GOSD is calculated as follows:[1]

$$\frac{{\rm d}f(K,E)}{{\rm d}E} = \sum_n \frac{E_n}{K^2} |\langle \Psi_n | \sum_{j=1}^{N} \exp({\rm i}\boldsymbol{K}\cdot\boldsymbol{r}_j) | \Psi_0 \rangle|^2 \delta(E_n - E).$$

Here, Ψ_0 and Ψ_n are the electronic wavefunctions of the initial and the final states, respectively, N is the anticipated number of electrons in the target particle, E_n is the excitation energy, and $\boldsymbol{r}_j$ is the position of the jth electron.

3. Results and discussion

The present absolute OOSD spectrum of CO is shown in Fig.1 along with that determined by the same method as ours but with a higher impact energy of 8 keV and a lower energy resolution of 1 eV (FWHM).[9] The calculated photoionization OOSD spectrum is also shown in Fig.1. Clearly, the present experimental results are in good agreement with those in Ref.[9] above 20 eV. The expanded spectrum below 20 eV is shown in the inset in Fig.1, and the discrepancy can be attributed to the difference in energy resolution. The present calculated results are generally in agreement with the experimental ones except for those below 17 eV (see the inset). This discrepancy is mainly due to the fact that the contribution from the autoionization Rydberg states is not included in our calculations. In addition, our calculations are based on self-consistent calculations, thus, electron correlation (i.e. channel interactions) is ignored.

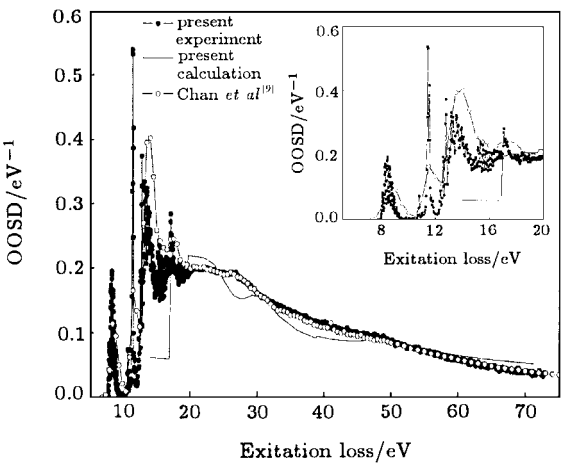


Fig.1. Absolute OOSD spectra of CO in an energy range of 5–75 eV. The inset exhibits the expanded spectrum in an energy range of 5–20 eV.

Figure 2 shows the absolute DDCS spectra below 120 eV at scattering angles of 0°, 2°, 4°, 6°, and 8°, which are equivalent to the Bethe surface. It can be seen clearly that the energy positions of the very broad peaks observed at 6° and 8° disperse to the side of higher energy loss with the increase of the momentum transfer. This ridge is the result of the momentum conservation in inelastic electron–molecule collision, and it is well known as the Bethe ridge in the first Born approximation.[1] Such a phenomenon has also been observed in other molecules such as NO,[7] O_2,[8] H_2O,[35] SF_6,[36] CF_3Cl, CF_2Cl_2, $2CFCl_3$,[37] and SiF_4.[38] The energy dispersion of this ridge with respect to K is generally related to the manifestation of different Fourier-transform components of the overlap density between the initial-state and final-state wave functions.[1] The Bethe surface gives us a clear perspective of the entirety of inelastic collisions.[1] Here we are interested in some peaks marked as A, B, and C , which stand out as K^2 increases. These peaks are discussed in detail in the order of excitation energies.

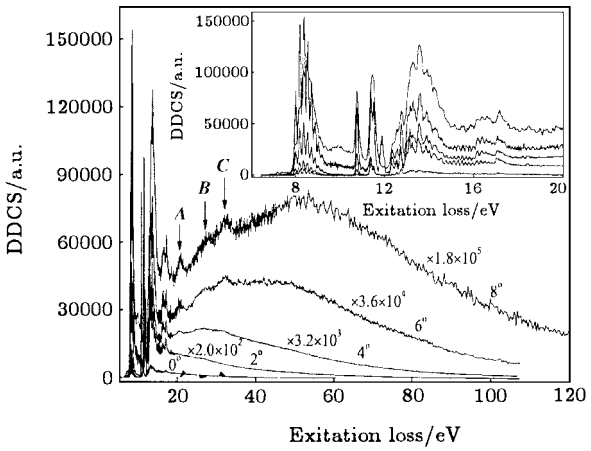


Fig.2. DDCS spectra measured at 0°, 2°, 4°, 6°, and 8°. The inset exhibits the expanded spectra in an energy range of 6–20 eV.

First, we discuss the peak A in a range of 19.67–23 eV in Fig.2, which is overwhelmed at 0° but stands out at 8°. Using the same method as ours but with a lower energy resolution (2.5 eV), Lee[18] has also observed the peak A at a large momentum transfer K and he suggested that the peak A was related to two electron transitions. In fact, the removal of an electron from the 5σ, 1π, 4σ and 3σ orbitals produces the following electronic states of CO^+(vertical ionization potentials in parentheses): $X^2\Sigma^+$(14.5 eV), $A^2\Pi$(17.2 eV), $B^2\Sigma^+$(20.1 eV) and $^2\Sigma^+$(38.9 eV).[23] Therefore, the peak A should be related to doubly excited states. Moreover, the assignments from fluorescence spectra[13–16] for the energy levels in an energy range of 18–30 eV are shown in Fig. 3(b). Clearly, the peak A is related to the doubly excited Rydberg series $(1\pi)^{-1}(5\sigma)^{-1}(2\pi)^1ns, np(n = 3, 4)$ and $(4\sigma)^{-1}(5\sigma)^{-1}(2\pi)^1ns(n = 3 - 6)$, respectively.[11–16] Figure 3(c) shows the photon-induced fluorescence spectra of CO from the neutral dissociation fragments in a wavelength range of 100–200nm.[15] Clearly, our measured profile of the spectrum in the energy range of 18–30 eV is different from that of the photon-induced fluorescence spectrum. For example, the maximum position of our spectrum, i.e. 20.8 eV, is about 0.9 eV lower than that of the fluorescence spectrum. This difference is understandable: our measured DDCS spectra include the contributions from all possible decay processes for a specific state, and the photon-induced fluorescence spectrum is only related to the neutral dissociation process and limited by the neutral photodissociation thresholds. Therefore, those states lower than neutral dissociation thresholds can not have such neutral dissociation decay paths, and can not be detected by the photon-induced fluorescence spectroscopy. However, the cross sections of other decay paths, such as autoionization, can be detected by the electron-impact method.

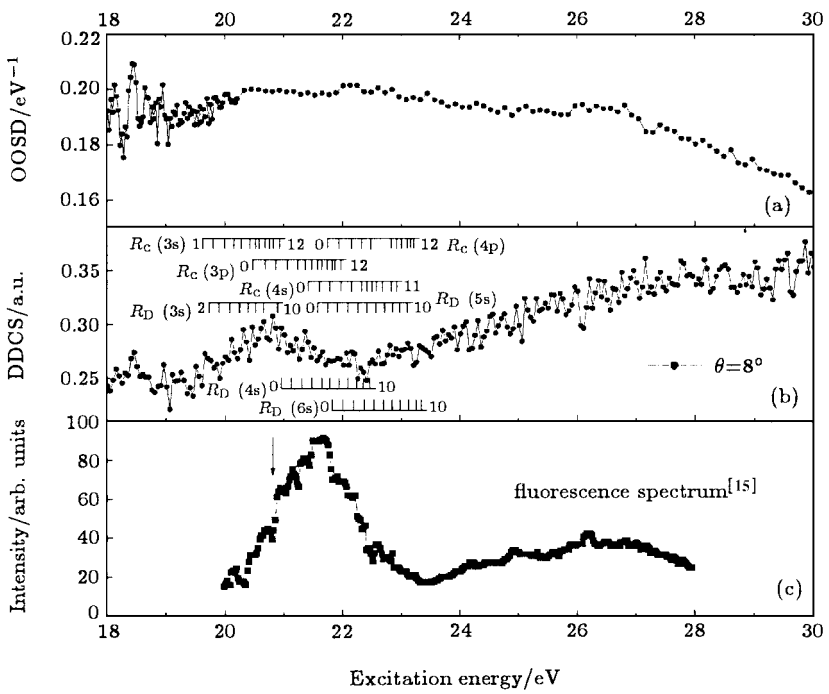


Fig.3. The spectra and assignments of CO in an energy range of 18–30 eV (a) OOSD; (b) DDCS measured at 8°; (c) fluorescence spectrum.

The peak B located at around 27.1 eV in Fig.2 is not clearly observed until the scattering angle reaches 4° ($K^2 \sim 0.9$a.u.). Using synchrotron radiation, Wu[10] have observed three weak peaks located at 27.01, 27.48 and 27.68 eV, respectively, in the absorption spectrum of CO, and Wu assigned them to the doubly excited Rydberg series converging to $F^2\Pi$ of CO^+. $F^2\Pi$ may have the configurations of $(4\sigma)^{-1}(5\sigma)^{-1}(2\pi)^1 n$p and $(5\sigma)^{-2}(2\pi)^1 n$p ($n = 4, 5, 6$).[10] Therefore, the peak B is related to the doubly excited Rydberg series. Generally, the first member of a Rydberg series has the strongest intensity, therefore, the maximum for the peak B is at 27.1 eV which may be corresponding to the energy position for $(4\sigma)^{-1}(5\sigma)^{-1}(2\pi)^1$4p and $(5\sigma)^{-2}(2\pi)^1$4p. Lee[18] did not find any structures in this energy region due to their low energy resolution (2.5 eV).

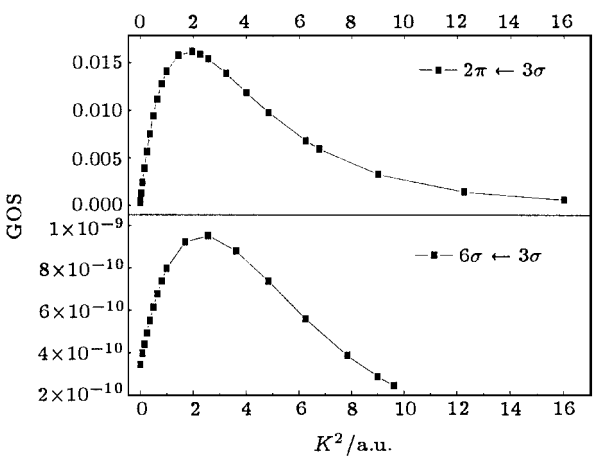


Fig.4. The GOS of $2\pi \leftarrow 3\sigma$ and $6\sigma \leftarrow 3\sigma$ as a function of K^2.

The peak marked as C at around 32 eV is not clearly observed until the scattering angle reaches 6° ($K^2 \sim 2$ a.u.). This peak has also been observed[18] and supposedly assigned to the transition of $(3\sigma)^{-1}(2\pi)^1 {}^1\Pi \leftarrow X^1\Sigma^+$ or $(3\sigma)^{-1}(6\sigma)^1 {}^1\Sigma^+ \leftarrow X^1\Sigma^+$. In order to elucidate the experimental observations, we plotted the GOS's curve versus K^2 for the excitation energies of $2\pi \leftarrow 3\sigma$ and $6\sigma \leftarrow 3\sigma$ based on the MSSCF method, which are shown in Fig.4. The calculated GOS's of $2\pi \leftarrow 3\sigma$ and $6\sigma \leftarrow 3\sigma$ reach the maximum in the K^2 range of 1.5–3.54a.u., i.e. in the scattering angle range of 5.2°–8°. The calculations are in agreement with the experimental observations. The calculated excitation energies of $2\pi \leftarrow 3\sigma$ and $6\sigma \leftarrow 3\sigma$ are 31.41 eV and 34.91 eV, respectively. The former is closer to the experimental one than the latter. The calculated GOS value of $2\pi \leftarrow 3\sigma$ is much larger than that of $6\sigma \leftarrow 3\sigma$. Therefore, we assign this peak to the transition of $(3\sigma)^{-1}(2\pi)^1 {}^1\Pi \leftarrow X^1\Sigma^+$. In fact, for an inner-valence transition, the behaviour in which GOS increases with momentum transfer K increasing up to the maximum of around 2a.u. in the K^2 range and then decreases with momentum transfer K, has also been observed in NO and O_2 molecules.[7,8]

4. Conclusion

The electron-energy-loss spectra of CO have been measured at the scattering angles of 0°, 2°, 4°, 6°, and 8° below 120 eV. Then the absolute OOSD spectrum and the absolute DDCS spectra have been determined. Peaks marked as A, B, and C above the first ionization threshold become prominent as K^2 increases. Based on previous work,[10–16,18] the peak A is assigned to the doubly excited Rydberg series $(1\pi)^{-1}(5\sigma)^{-1}(2\pi)^1 n$s, np($n = 3, 4$) and $(4\sigma)^{-1}(5\sigma)^{-1}(2\pi)^1 n$s($n = 3 - 6$), respectively. Since our measured DDCS spectra include the contributions from all possible decay processes for a specific state, and the photon-induced fluorescence spectrum is only related to the neutral dissociation process, the profile of peak A in the present work is different from that of fluorescence spectra (see Fig.3). The peak B is assigned to the doubly excited states that have the configuration of $(4\sigma)^{-1}(5\sigma)^{-1}(2\pi)^1$4p and $(5\sigma)^{-2}(2\pi)^1$4p. Based on our calculations, we not only assign the peak C at around 32 eV to the inner-valence transition of $(3\sigma)^{-1}(2\pi)^1 {}^1\Pi \leftarrow X^1\Sigma^+$ but also quantitatively explain why the peak C stands out as K^2 increases (see Fig.4). In summary, the reported superexcited states below 120 eV for CO are almost observed in the present work. AREELS is an important method supplementary to the three most commonly used methods to investigate the structure of superexcited states, because AREELS includes all possible decay processes for a specific state, and some superexcited states may stand out as K^2 increases.

References

[1] Inokuti M 1971 *Rev. Mod. Phys.* **43** 297

[2] Bethe H 1930 *Ann. Phys.* (Leipzig) **5** 325
Bethe H 1930 *Z. Phys.* **76** 293

[3] Platzman R L 1962 *Radiat. Res.* **17** 419

[4] Platzman R L 1962 *Vortex* **23** 372

[5] Hatano Y 1999 *Phys. Rep.* **313** 109

[6] Zhong Z P, Han X Y, Zhang W H and Li J M 2004 *Chin. Phys. Lett.* **21** 279

[7] Sun J M, Zhong Z P, Zhu L F, Li W B, Liu X J, Yuan Z S and Xu K Z 2004 *Phys. Rev.* A **70** 012708

[8] Fan L L, Zhong Z P, Zhu L F, Liu X J, Yuan Z S, Sun J M and Xu K Z 2005 *Phys. Rev.* A **71** 032704

[9] Chan W F, Cooper G and Brion C E 1993 *Chem. Phys.* **170** 123

[10] Wu C Y R 1982 *J. Chem. Phys* **77** 1179

[11] Colding K and Potts A W 1974 *J. Phys.* B **7** 163

[12] Álvarez Ruiz J, Erman P, Rachlew-Källne E, Rius i Riu J, Stankiewicz M and Veseth L 2002 *J. Phys.* B **35** 2975

[13] Erman P, Rachlew-Källne E and Sorensen S L 1994 *Z. Phys.* D **30** 315

[14] Ehresmann A, Machida S, Ukai M, Kameta K, Kitajima M, Kouchi N, Hatano Y, Ito K and Hayaiski T 1995 *J. Phys.* B **28** 5283

[15] Ehresmann A, Machida S, Ukai M, Kameta K, Kitajima M, Kouchio N, Hatano Y, Ito K and Hayaishi T 1996 *J. Phys.* B **29** 3629

[16] Ehresmann A, Machida S, Ukai M, Kameta K, Kitajima M, Kouchio N, Hatano Y, Ito K and Hayaishi T 1997 *J. Phys.* B **30** 1907

[17] Dadouch A, Dujardin G, Hellner L and Besnard-Ramage M J 1991 *Phys. Rev.* A **43** 6057

[18] Lee J S 1977 *J. Chem. Phys* **67** 3998

[19] Sun J M, Zhong Z P, Zhu L F, Liu X J, Yuan Z S and Xu K Z 2005 *Chin. Phys.* **14** 1378

[20] Xu K Z, Feng R F, Wu S L, Ji Q, Zhang X J, Zhong Z P and Zheng Y 1996 *Phys. Rev.* A **53** 3081

[21] Liu X J, Zhu L F, Jiang X M, Yuan Z S, Cai B, Chen X J and Xu K Z 2001 *Rev. Sci. Instrum.* **72** 3357

[22] Wu S L, Zhong Z P, Feng R F, Xing S L, Yang B X and Xu K Z 1995 *Phys. Rev.* A **51** 4494

[23] Huber P and Herzberg G 1979 *Molecular Spectra and Molecular Structure* Vol.4 (Princeton, NJ: Van Nostrand)

[24] Chan W F, Cooper G and Brion C E 1991 *Phys. Rev.* A **44** 186

[25] Zhong Z P, Zhang W H, Xu K Z, Feng R F and Li J M 1999 *Acta Phys. Sin.* **48** 816 (in Chinese)

[26] Zhu L F, Zhong Z P, Ji Q, Zhang X J, Wu S L, Feng R F and Xu K Z 1997 *Acta Phys. Sin.* **46** 458 (in Chinese)

[27] Olney T N, Cann N M, Cooper G and Brion C E 1997 *Chem. Phys.* **223** 59

[28] Wheeler J A and Bearden J A 1934 *Phys. Rev.* **46** 755

[29] Dehmer J, Inokuti M and Saxon R P 1975 *Phys. Rev.* A **12** 102

[30] Sze K H, Brion C E, Tong X M and Li J M 1987 *Chem. Phys.* **115** 433

[31] Pan X C, Liang X L and Li J M 1987 *Acta Phys. Sin.* **36** 426 (in Chinese)

[32] Liu L and Li J M 1991 *J. Phys.* B **24** 1893

[33] Tong X M, Li J M, Sze K H and Brion C E 1987 *14th International Conference on X-ray Inner-shell Processes* (Paris)

[34] Tong X M and Li J M 1989 *J. Phys.* B **22** 1531
Tong X M and Li J M 1989 *16th ICPEAC* (New York)

[35] Dingfelder M and Inokuti M 1999 *Radiat. Environ. Bioph.* **38** 93

[36] Turci C C, Francis J T, Tyliszczak T, de Souza G G B and Hitchcock A P 1995 *Phys. Rev.* A **52** 4678

[37] Leung K T 1999 *J. Electron Spectrosc. Relat. Phenom.* **100** 237

[38] Fan X W and Leung K T 2001 *J. Chem. Phys.* **115** 2603